N O T I C E

THIS DOCUMENT HAS BEEN REPRODUCED FROM
MICROFICHE. ALTHOUGH IT IS RECOGNIZED THAT
CERTAIN PORTIONS ARE ILLEGIBLE, IT IS BEING RELEASED
IN THE INTEREST OF MAKING AVAILABLE AS MUCH
INFORMATION AS POSSIBLE

EVALUATION AND DEVELOPMENT OF SATELLITE INFERENCES OF
CONVECTIVE STORM INTENSITY USING COMBINED CASE STUDY
ANALYSIS AND THUNDERSTORM MODEL SIMULATIONS

by

William R. Cotton
Gregory J. Tripoli

First-Year Report to Severe Storms Research
National Aeronautics and Space Administration
Washington, D.C.   20546

Grant No. NSG 5341
Period: 1 May, 1979 - 30 April, 1980

Department of Atmospheric Science
Colorado State University
Fort Collins, CO 80523

July, 1980

7/16/80 CC. NSTIF
(T.O. HAS A copy)

JUL 0 8 1980
RECEIVED
NASA STI FACILITY
ACCESS DEPT.

1.0 INTRODUCTION

In this report we summarize major research accomplishments that have been achieved under support of NASA Grant No. NSG 5341 during the first year of the grant. The research has concentrated in the following areas:

i) an examination of observational requirements for predicting convective storm development and intensity as suggested by recent numerical experiments

ii) interpretation of recent 3D numerical experiments with regard to the relationship between overshooting tops and surface wind gusts

iii) the development of software for emulating satellite-inferred cloud properties using 3D cloud model-predicted data

iv) the development of a conceptual/semi-quantitative model of eastward propagating, mesoscale convective complexes forming to the lee of the Rocky Mountains.

2.0 OBSERVATIONAL REQUIREMENTS FOR PREDICTING CONVECTIVE STORM DEVELOPMENT AND INTENSITY AS SUGGESTED BY RECENT NUMERICAL EXPERIMENTS

In the December 1979 Interim Progress Report on this Grant, we concluded, based on modeling experience at that time, that the following observations are needed for the "precise" prediction of the time and location of convective storm development, and the intensity and movement or propagation of convective storms:

i) the magnitude of low-level, mesoscale convergence of mass and moist static energy

ii) the vertical distribution of mesoscale convergence

iii) vertical profiles of the horizontal wind with special emphasis on the lower one-third of the cloud layer and the temporally varying sub-cloud layer

iv)   a definition of mesoscale convergence "anomaly producers".

Since that time, two sets of numerical experiments have been in progress. The first experiment discussed more thoroughly in section 3.0 and Appendix 1 involves the simulation of a Florida towering cumuli and its dynamic response to seeding. The second experiment described by Cotton, Tripoli and Knupp (1980: Appendix 2), involves the simulation of the development and organization of a quasi-steady thunderstorm over South Park, Colorado. The mesoscale features affecting the formation of this storm have been described by George (1979) and the detailed morphology of the storm has been described by Knupp (1980). The results of these numerical experiments support the conclusions derived from earlier experiments and add new insight into environmental factors contributing to convective storm development, and the intensity and movement or propagation of convective storms.

The "dynamic seeding" experiments discussed in section 3.0, suggest that the intensity of surface wind gusts and their subsequent impact on convective storm propagation are strongly modulated by the vigor and thermodynamic consequences of entrainment. The vigor of entrainment, in turn, is largely controlled by the strength of vertical shear of the horizontal wind and by vertical stretching of the updraft as a consequence of explosive growth. Also, for a given amount of entrainment, the amount of cooling is a function of the dryness of the environmental air at the levels of maximum entrainment.

Some of the environmental factors contributing to explosive growth or vertical stretching of an updraft are discussed in section 3.0. Since strong shear and dryness of lower, mid-tropospheric air favor vigorous entrainment and, thusly, strong surface wind gusts, these simulations

support the severe weather forecaster's use of minimum θ_e and shear intensity as indices of thunderstorm wind gust intensities. In fact, other things being the same (i.e., factors contributing to explosive growth), one would expect that the favored source level of downdraft air would be the region where the minimum in θ_e and the maximum in vertical wind shear coincide. Strong shear thus would favor the initiation and maintenance of entrainment at a given level, while a minimum in θ_e would favor strong evaporation which initiates and maintains a vigorous downdraft.

The attempts to simulate the quasi-steady thunderstorm analyzed by Knupp (1980) have been quite frustrating. It appears that the scenario of prior convective activity over South Park and the horizontal inhomogeneity of the mesoscale convective gust frontal air, all contribute to creating the unique organization of the observed storm. A number of modelers have speculated that continuously propagating storm systems should lose their memory of the cloud initiating mechanism once the main updraft/downdraft couplet becomes well established. In this case, however, the observed wind field led to continuous propagation on the N.E. flank; whereas it was observed to propagate on its N.W. flank. It appears from George's (1979) mesoscale analysis that flow diverted around earlier cells could have created an initial N.W. flow at low levels that would have initiated propagation on that flank. These results suggest that observations of horizontal inhomogeneities in low level flow on the mesoscale are needed to uniquely predict a given convective storm.

3.0 OVERSHOOTING TOPS AND SURFACE WIND GUSTS OR DOWNBURSTS

Recently, Cotton, et al. (1980; Appendix 1) have applied the CSU, 3D cloud model to the simulation of the dynamic response of a Florida cumulus

to seeding. This particular version of the model contains an ice-phase parameterization developed by Stephens (1979). The numerical experiments were designed to investigate the cloud dynamic responses to artificially-induced "explosive growth". Seeding was accomplished by setting the ice crystal concentration at $100\ell^{-1}$ for a period of 10 minutes over the $-5°$ to $-10°C$ range and over a horizontal area which constituted the core of the rising tower.

As a consequence of seeding, updraft speeds increased from $15m\ s^{-1}$ to $33m\ s^{-1}$ and the cloud exhibited strong overshooting into the stratosphere. The cloud penetrated up to 13.9 km MSL and developed strong negative buoyancies of up to $-6°C$ at 13 km MSL. Since vigorous tropospheric over-shooting was simulated in this case, it seemed reasonable to expect that further analysis of this simulation may shed light on the relationships between overshooting and surface wind gusts. One would not expect that the intensity of surface wind gusts in the Florida environment to approach "downburst" (see Fujita and Byers, 1977), magnitudes, nonetheless the mechanisms of communication between tropospheric overshooting and surface gusts should be similar.

In the seeded cloud simulation, a downdraft reaching down to the surface was predicted, with maximum values of $10.5m\ s^{-1}$ at a height of 1500m and $5.9m\ s^{-1}$ at 750m, and an associated maximum horizontal divergence at 0.4 km of $1.24 \times 10^{-2}s^{-1}$. Not surprisingly, this does not quite meet Fujita and Byer's (1977) definition of a downburst as "a localized intense downdraft with vertical currents exceeding a downward speed of 12 ft s^{-1} ($\sim 4m\ s^{-1}$) at 300 ft ($\sim 100m$) above the surface." This value corresponds to a point divergence of $4 \times 10^{-2}\ s^{-1}$. However, these downdraft velocities are significant enough to warrant a closer look at the dynamic links between

overshooting tops and downdrafts.

In the seeded cloud simulation, the overshooting top first manifests itself after 2800s of simulated time. At that time, the cloud possesses a negative buoyancy of $-1^{\circ}C$ at 11.6 km. The top continues to rise until it reaches a height of 13.9 km at 3000s. It then collapses back, as exemplified by a maximum downdraft value of 2.3m s^{-1} at 13.9 km, 100s later. A peak downdraft magnitude of 9.9m s^{-1} in the upper troposphere occurs at 3400s at an altitude of 10.1 km. This is considerably less than the 41m s^{-1} sinking speeds of the collapsing tops reported by Fujita (1974), however.

Fujita and Byers (1977) hypothesized the following cell model to explain the dynamic linkage between overshooting tops and surface wind gusts (downbursts). The model involves tops overshooting the anvil then collapsing into a strong downdraft (located at approximately 10 km) and trail of precipitation. Entrainment at the top transports dry air and large horizontal momentum downward. Ice crystals are hypothesized to rapidly sublime in the subsaturated entrained air, thereby taking up heat from the air resulting in a cold, negatively buoyant downdraft. The collapsing top and entrained air accelerate the train of precipitation and import fast horizontal momentum from the stratosphere. A successive rise and fall of the top will create a family of downburst cells that moves away from the parent thunderstorm.

In our simulation, it is not possible to explain the low-level downdraft at 1500m, which exceeds 10m s^{-1} at 3000s, as the extension of the downward motion at cloud top. A very crude trajectory estimate employing maximum downdraft velocities for a given height and time, places an upper limit of about 5 km for the source level of the sub-cloud downdraft air. The bulk of the downdraft air originates from levels substantially below

that, as can be seen from cross sections of the flow field. Both numerical simulations (Miller, 1978; Tripoli and Cotton, 1980) and observational studies (Kropfli and Miller, 1976; Brandes, 1977) have shown that sub-cloud convective downdrafts originate at midlevels, and not at the tropopause level. It thus seems that we can consider the results of this study to be of more general validity.

The fact that in the "no-seed" simulation both sub-cloud downdrafts and overshooting tops were much less pronounced than in the "seed" simulation suggests there is a linkage between overshooting tops and surface wind gusts (downbursts), although different from that envisaged by Fujita and Byers. Based on the dynamic differences between the simulated seeded and nonseeded clouds, the following model is proposed.

Associated with the additional release of latent heat in the seeded cloud region is a buoyancy pulse which leads to "explosive" vertical growth. One consequence of this increased vertical momentum is the strong overshooting into the stratosphere (see Fig. 1). Another consequence of the "explosive" tower growth is the vertical mass flux divergence at and below the seeding level, which leads to dynamic entrainment of dry environmental air. The strong dynamic entrainment is clearly evident in Fig. 1 as well as in the horizontal cross section at 4.9 km shown in Fig. 2. As evidenced by the cut off tower, the model appears to overpredict the rate of dynamic entrainment. This is probably a consequence of the design of the seeding routine or to the fact that the present model formulation requires that a grid volume be wholly saturated or unsaturated whereas the entrained region can be expected to be composed of fluctuating saturated and unsaturated blobs of air.
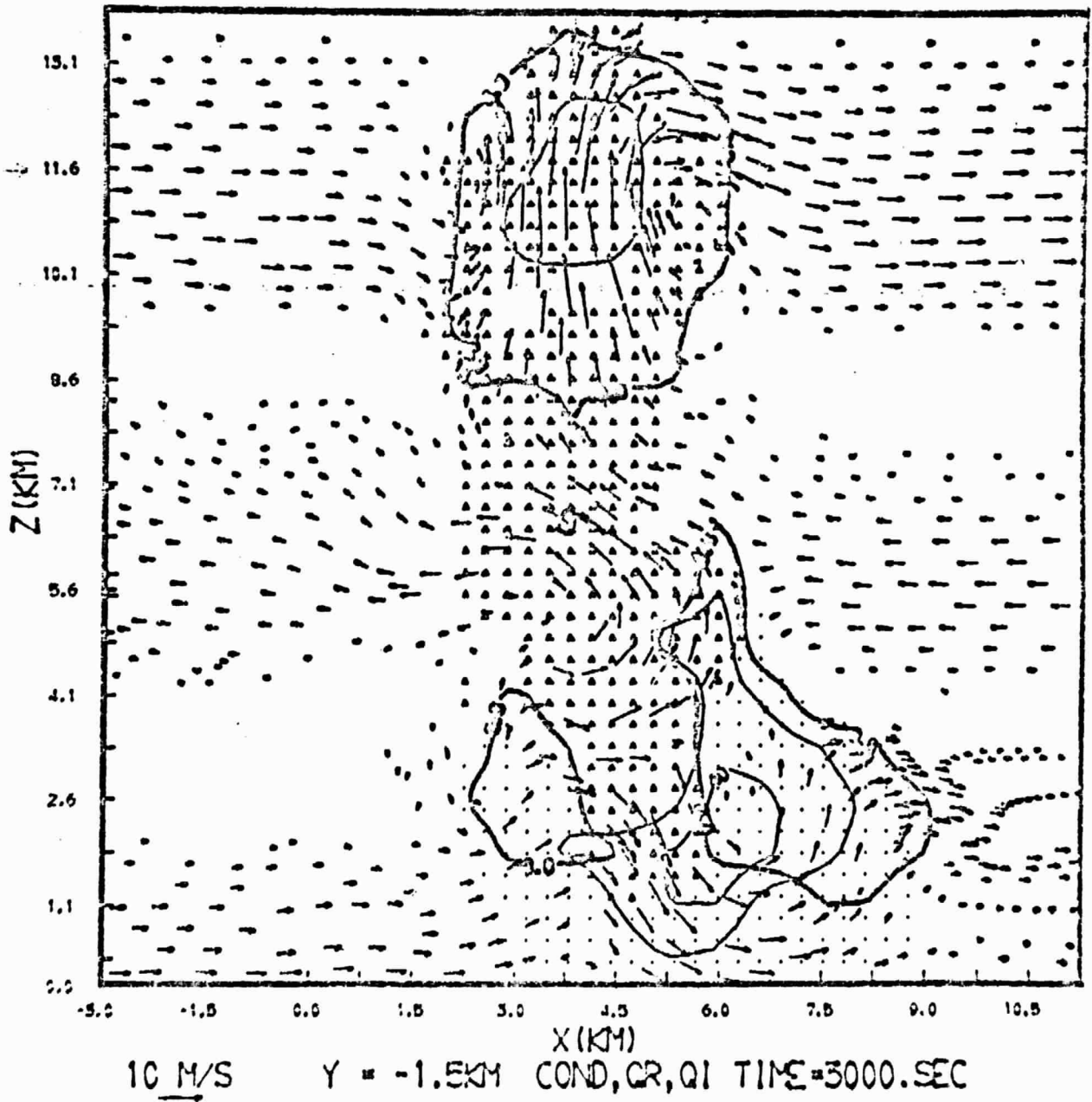
FACE CASE STUDY (EXPERIMENT K)

Figure 1

FACE CASE STUDY (EXPERIMENT K)
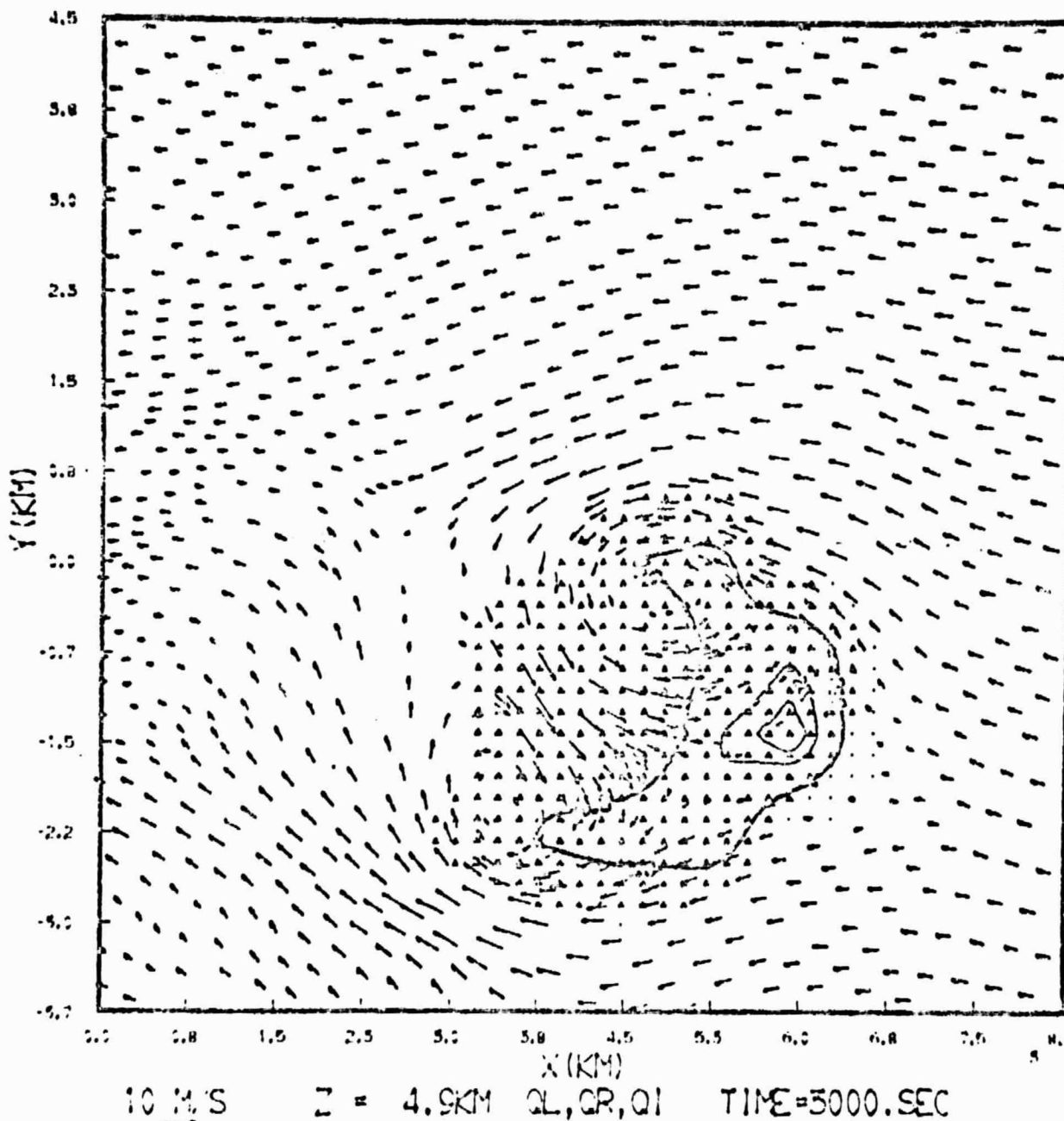
10 _M/S   Z = 4.9KM   QL, QR, QI   TIME=3000.SEC

Figure 2

As a consequence of the dynamic entrainment of dry environmental air, evaporational cooling, together with the load of liquid water, lead to the formation of a downdraft. The downdraft subsequently descends to the surface being continually reinforced by evaporation of cloud droplets and precipitation and by water loading. Thus, the basic mechanism linking overshooting tops and surface wind gusts is dynamic entrainment associated with vertical mass flux divergence due to "explosive growth".

One is led to ask, therefore, what are the factors that naturally lead to "explosive growth" and its dynamic consequences? The modeling experiments briefly described herein, as well as those reported by Tripoli and Cotton (1980) suggest that explosive cloud development is strongly favored by the presence of mesoscale convergence and by anomalies in subcloud vertical motion on the cloud-scale. It is interesting to note that the case reported by Fujita and Byers involved the particpitation of a sea breeze convergence line as well as an intersecting arc cloud (gust front) which provides both the necessary mesoscale and cloud-scale forcing mechanisms.

The numerical experiments reported by Cotton (1972) also suggest that the microphysical factors favoring explosive growth would be a suppression of a warm cloud precipitation process (collision and coalescence) until a tower penetrates deep into the supercooled layer. This would allow the vertical transport of large quntities of supercooled water which is then available for subsequent freezing and latent heat release. If the liquid-liquid collision and coalescence process then commences, a volatile mixture of supercooled raindrops and an exponentially increasing concentration of ice crystals (as the tower rises and cools in the supercooled region) can lead to the rapid and complete glaciation of the rising tower. The

subsequent release of latent heat would lead to explosive growth in a manner analogous to our seeding simulation.

There are several ramifications of this model of the linkage between overshooting tops and surface wind gusts. First of all, from a now-casting point of view, the satellite detection of an overshooting top would provide little lead time to the desemination of surface wind gust or downburst warnings. This is because the formation of the overshooting top would occur in concert with the formation of a vigorous downdraft in the lower troposphere. Secondly, to forecast downbursts or several wind gusts the emphasis should shift from interpreting upper tropospheric environmental properties favorable for downdraft formation to lower, mid-tropospheric properties. Clearly, strong vertical shear of the horizontal wind in the lower, mid-troposphere would favor vigorous entrainment. Furthermore, low values of 0_e in the same region would favor vigorous evaporation of cloudy air in the entrained regions.

Clearly this work represents only a small step forward in our understanding of the factors contributing to explosive growth and the linkages between explosive growth in the upper troposphere and surface wind gusts or downbursts. It would certainly be desirable to extend this research by simulating explosive growth in an actual downburst-producing environment.

4.0 THE DEVELOPMENT OF SOFTWARE FOR EMULATING SATELLITE-INFERRED CLOUD PROPERTIES USING 3D CLOUD MODEL-PREDICTED DATA

Before leaving our group and joining G.E. MATSCO to work with NASA, Mr. Mark Stephens began the development of algorithms to emulate the analysis of satellite-derived cloud top isotherms using data predicted with the 3D cloud model. The algorithm involves a search for cloud top and mapping of a satellite plane of data (i.e., cloud top temperature). Using data

predicted by the model in its non-icephase version, he then computed the rate of expansion of isotherm area $\left(\dfrac{d \ln A}{dt}\right)$.

Stephens then compared the predicted $\dfrac{d \ln A}{dt}$ to the predicted horizontal velocity divergence D. The divergence was computed at the height having an average horizontal temperature corresponding to the isotherm used in calculating $\dfrac{d \ln A}{dt}$. Also, the D was evaluated over the area of the isotherm projected onto the plane on which D is to be computed.

The rate of isotherm expansion was also compared with predicted total eddy kinetic energy and the location and amplitude of maximum updraft speed as well as precipitation intensity.

In the test case, Stephen's found generally poor correspondence between $\dfrac{d \ln A}{dt}$ and D. The best correlation occurred at the time that the storm was at its peak kinetic energy early in the cloud's life history (30 to 40 min). After this time, other factors affecting isotherm expansion became more influential. Some of these factors were model dependent, especially for the stage of model development at that time. Factors affecting isotherm expansion other than velocity divergence include:

1) The anvil not only expands outward from a central point, but also extends its area by cloud water condensing or moving upward through a region. This effect can be expected to be of greater importance when the ice-phase is included in the model predictions.

2) Since the anvil is composed of cloud water, it is more influenced by evaporation than a similar anvil composed of ice particles.

3) The above-mentioned evaporation of the anvil also leads to a disorganized anvil structure which contributes to a noisy estimate of $\dfrac{d \ln A}{dt}$.

The calculation of $\dfrac{d \ln A}{dt}$ must also be terminated when the anvil

reaches the lateral boundary of the model.

Mr. Dave Hahn (he has recently completed requirements for an M.S. degree) is now continuing the development of algorithms emulating satellite views of convective storms. This work will make use of model-predicted data in which the ice phase is included in the model (see sections 2.0 and 3.0).

5.0 DEVELOPMENT OF A CONCEPTUAL/SEMI-QUANTITATIVE MODEL OF EASTWARD PROPAGATING, MESOSCALE CONVECTIVE COMPLEXES FORMING TO THE LEE OF THE ROCKY MOUNTAINS

The development of a conceptual/semi-quantitative model of eastward propagating, mesoscale convective complexes has been concentrated on the analysis of convective complexes forming during the period 3 August to 10 August, 1977. A two-part paper is now being prepared for submission to the Monthly Weather Review entitled: A Long-Lived Mesoscale Convective Complex, Part I - The Mountain Generated Component, and Part II - Morphology of the Mature Complex.

Part I is basically a synthesis of George's (1979) thesis. The paper follows a scenario of convective envolution from the early morning micrometeorological scale, to the mid-day ridge/valley circulation and mountain cumuli/cumulonimbus, to mid-afternoon plains cumulonimbus and squall lines, to the formation of a mesoscale convective complex (MCC).

In Part II, the pre-MCC synoptic field is re-analyzed and the morphology of the MCC is described including:

i) the interaction of the MCC with the remains of the previous day's MCC

ii) the intrusion of dry, high momentum air into the back of the storm at 500 mb

iii) a broad region of high momentum outflow from the storm just below the tropopause

iv) a significant meso-anticyclone at 200 mb which was not present prior to the formation of the MCC

v) lack of direct interaction with the polar front jet well to the north

vi) divergence profiles similar to tropical clusters

vii) virtually no evidence of poleward meridional heat transport associated with the MCC as one would expect in a baroclinic system.

It is concluded that the MCC's studied are basically tropical in nature and their dynamics are dominated by buoyant accelerations. Associated weak baroclinic features, such as a surface stationary front, serve to trigger and direct the release of convective instability. It is suggested from this analysis that a certain amount of baroclinicity may be compatible with an MCC, but as the baroclincity increases the convection either tends to organize itself into the linear structure of a squall line or the system as a whole undergoes a transformation into a rapidly occluding cyclonic wave.

Dr. Pete Wetzel is a major contributor to Part II of these papers, therefore our goal is to complete these manuscripts before Dr. Wetzel joins the NASA/GLAS Severe Storms Group in Sept. 1980.

6.0 REFERENCES

Brandes, E.A., 1977: Flow in severe thunderstorms observed by dual-Doppler radar. Mon. Wea. Rev., 105, 113-120.

Cotton, W.R., 1972: Numerical simulation of precipitation development in supercooled cumuli, I & II. Mon. Wea. Rev., 100, 757-784.

Cotton, W.R., T. Nehrkorn, G. Tripoli, and Jol 1 B. Cunning, 1980:
A three-dimensional simulation of the dynamic response of a Florida
cumulus to seeding. Third WMO Scientific Conference on Weather Modi-
fication, Clermont-Ferrand, France, 21-25 July, 1980.

Cotton, W.R., G.J. Tripoli, and K.R. Knupp, 1980: A three-dimensional
numerical simulation and observational analysis of an intense, quasi-
steady thunderstorm over mountainous terrain. VIIIth International
Conference on Cloud Physics, Clermont-Ferrand, France, 15-19 July,
1980.

Fujita, T. Theodore, and Horace R. Byers, 1977: Spearhead echo and down-
burst in the crash of an airliner. Mon. Wea. Rev., 105, 129-146.

George, Raymond L., 1979: Evolution of mesoscale convective systems over
mountainous terrain. M.S. thesis, Atmos. Sci. Paper # 318, Dept. of
Atmos. Sci., Colo. St. Univ., Ft. Collins, Colo., 160 pp.

Knupp, Kevin R., 1980: Observed characteristics of an intense, quasi-
stationary thunderstorm complex over mountainous terrain. M.S. thesis,
Dept. of Atmos. Sci., Colo. St. Univ., Ft. Collins, Colo., 196 pp.

Kropfli, R.A., and L.J. Miller, 1976: Kinematic structure and flux
quantities in a convective storm from dual-Doppler radar observations.
J. Atmos. Sci., 33, 520-529.

Miller, M.J., 1978: The Hampstead storm: A numerical simulation of a
quasi-steady cumulonimbus system. Quart. J. R. Met. Soc., 104,
413-427.

Stephens, Mark Argyle, 1979: A simple ice phase parameterization. M.S.
thesis, Atmos. Sci. Paper # 319, Dept. of Atmos. Sci., Colo. St.
Univ., Ft. Collins, Colo., 122 pp.

Tripoli, G., and W.R. Cotton, 1980: A numerical investigation of
several factors contributing to the observed variable intensity of
deep convection over South Florida. Submitted to J. Appl. Meteor.,
In press.

APPENDIX 1

A Three-Dimensional Simulation of the Dynamic Response
of a Florida Cumulus to Seeding

A THREE-DIMENSIONAL SIMULATION OF THE DYNAMIC RESPONSE

OF A FLORIDA CUMULUS TO SEEDING

W.R. Cotton, T. Nehrkorn and G. Tripoli
Department of Atmospheric Science
Colorado State University

John B. Cunning
National Hurricane and Experimental Meteorology Laboratory, NOAA
Coral Gables, Fla. 33146

1. Introduction

"Dynamic seeding" of convective clouds as it is being performed in the NOAA Florida
Area Cumulus Experiment (FACE) rests on the assumption that seeding of actively growing
towers will lead to a conversion of supercooled liquid water to ice and subsequent
"explosive growth" due to the latent heat release. The accelerated growth of rising
towers is then hypothesized to lead to strengthened low level inflow, subcloud layer con-
vergence and possibly even merger of neighboring clouds. It was pointed out by Cotton
and Tripoli (1979) and Simpson (1980) that downdrafts might play a key role in communi-
cating enhanced buoyancy at the -10°C level down to the subcloud layer.

The present study will attempt to provide answers to some of the questions raised
with respect to the dynamic response of a cumulus to seeding. A three-dimensional model
which includes an ice-phase parameterization is used to determine differences between a
seeded and unseeded cloud. In this paper, a short summary of the model is given, the case
study is described and the results of the numerical experiments are discussed.

2. Model Description

The three-dimensional cloud model employed in this study is a revised version of the
model reported by Cotton and Tripoli (1978) and Tripoli and Cotton (1980). Major changes
include the use of the quasi-conservative thermodynamic variable ice-water potential
temperature θ_i (Tripoli and Cotton, 1979) and the addition of an ice-phase parameterization
(Stephens, 1979). Some other major features of the model are:

1) it is fully 3D
2) it is non-hydrostatic, time-split compressible
3) it utilizes sigma-z vertical coordinate
4) it presently has "Smagorinsky-type" eddy viscosity, first-order turbulence closure
5) its lower boundary condition on turbulent fluxes is derived from a similarity
   theory based surface layer parameterization
6) it contains a simple rain parameterization using autoconversion and accretion
   assuming rain is distributed according to:

$$\phi(R) = \frac{N_R}{R_m} \; EXP \; (-R/R_m) \quad \text{with } R_m \text{ constant}$$

7) it contains an ice-phase parameterization developed by Stephens (1979)
8) the lower vertical boundary condition is given by a surface layer turbulence
   parameterization and zero mean advective fluxes. The top boundary is a 3 km
   deep Rayleigh friction layer capped by a rigid lid
9) the lateral boundary conditions are a variation on the Klemp-Wilhelmson (1978)
   radiative lateral boundary condition
10) it uses second-order finite differencing in space
11) its time differencing scheme is Matsuno (1966) on small time-steps and leap-frog
    with Asselin filter on long time-steps
12) its grid-spacing is 750 meters in the horizontal and vertical over a 36.75 x
    36.75 km (horizontal) x 15 km (vertical) domain
13) it is initialized with a base-state sounding, large-scale convergence and a
    dynamic focusing algorithm described by Tripoli and Cotton (1980).

3. Case Study Description and Design of Experiment

The numerical experiments are performed in an environment described by measurements
taken on the 25th of August 1975 as part of NOAA/Florida Area Cumulus Experiment(FACE).
Two convective systems formed inside the surface mesonetwork on that day. The second one
of these was an isolated system and is subject of a case study by Cunning et al. (1979).
It formed at about 1830 GMT and three of its growing towers were seeded with silver iodide
(AgI) by aircraft at 1834 GMT, 1838 GMT and 1840 GMT. Each tower was seeded when it
reached the -10°C level. Following seeding, a fourth (unseeded) tower grew explosively to
a higher level than either one of the three previous cells. Throughout its life-cycle,
the system was continuously scanned by triple Doppler radar.

The present study will not attempt to reproduce the features of any particular cloud,
but rather investigate the effects of seeding on a cloud of comparable dimensions in a
similar environment. Accordingly, the base state sounding used to initialize the model
is a modified 1745 GMT special sounding taken at the center of the observation network
matched with the Miami 1200 GMT sounding above 300 mb. The wind profile is composited
from low level PIBAL observations at the central observation site at 1745 GMT and Miami
1200 GMT rawinsonde data above that. To prevent the cloud from being advected out of the
domain, the low-level mean was removed. The sounding is conditionally unstable and
relatively dry above 700 mb. The vertical wind shear which is most pronounced in the
u-component can be seen from Figure 1. The imposed mean vertical motion field is based on
numerical model re lts by Pielke (personal communication) and is matched to an observed
value of surface convergence of 2×10^{-4} s^{-1}. Numerical values are 0.09 m s^{-1} at 750 m,
0.13 m s^{-1} at 1500 m, 0.10 m s^{-1} at 2250 m, 0.05 m s^{-1} at 3000 m and 0.02 m s^{-1} at 3750 m.
Twenty-eight percent of this convergence was focused on a scale of 2.25 km, resulting in a
peak vertical velocity of 3 m s^{-1} in the center of the domain. Experiment I was initialized
with this procedure. Experiment II is identical to Experiment I except that seeding is
simulated after 41 min 40 sec, at which time the cloud has reached the -10°C level. Based
on the number of flares released into the cloud system and their nucleation efficiency
(Sax et al., 1979) the total number of artificial nuclei was estimated. In consistency
with this estimate, the ice-nuclei concentration was set equal to 100 ℓ^{-1} over a period of
10 min for 2 levels in the vertical (-5°C to -10°C range) over a horizontal area which
constituted the core of the rising tower (3.75 km $\le x \le$ 5.25 km, and -1.5 km $\le y \le$ -.75 km).
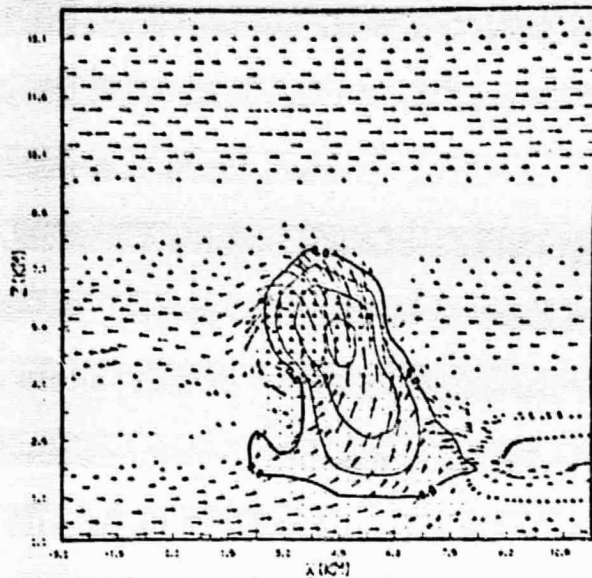
4. Results

Experiment I:

Due to the pure convergence initialization without any temperature or moisture per-
turbation the initial growth of the cloud is fairly slow. At 30 min, the cloud reached
a cloud top height of 4 km, after which time the cloud top rises by about 5 m s^{-1}. The
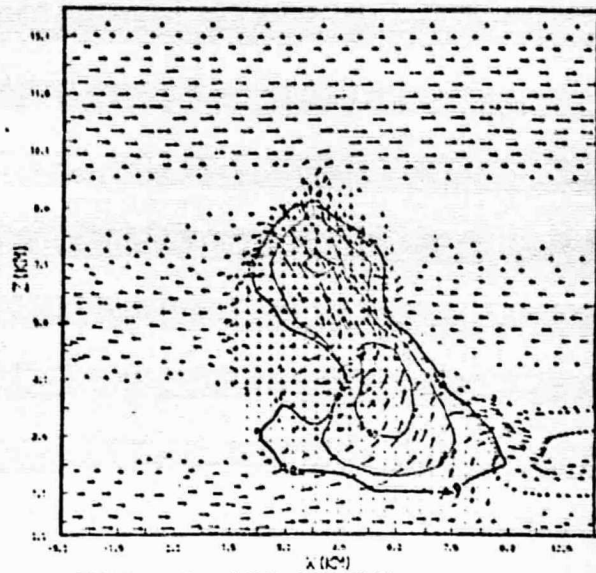vertical wind shear leads to a tilted updraft and strong entrainment of dry air on the

Fig. 1: Cloud development at a) 45 minutes and b) 50 minutes. The thick solid line marks the cloud outline, thin solid lines are contours of total condensate (every 2 g kg^{-1}). The presence of rainwater and graupel is denoted by a dot or a triangle, respectively.

downshear side of the cloud (Fig. 1). After one hour, the rising tower is completely cut off from its low-level support and rises in a bubble-like fashion up to the tropopause. The "time-window" effect for seeding potential is evident from the fact that virtually all the supercooled liquid water at the -10°C level is frozen within a time period of less than 10 min. In comparison with the observations, it should be noted that due to the limited resolution of the model, only one large rising tower is reproduced rather than four individual cells.

Experiment II:

"Seeding" the rising tower not only resulted in a complete glaciation of the cloud throughout the seeded volume mainly by conversion of liquid water to graupel, but produced marked dynamic changes as well. Updraft speeds increased from 15 m s^{-1} to 33 m s^{-1} and the updraft widened and deepened. The correlation between vertical explosive growth and widening of the cloud was documented by Simpson, et al. (1965) and Simpson, Brier and Simpson (1967). The pressure minimum at middle levels associated with the updraft was much more pronounced following seeding while at the same time pressure increased slightly below cloud base. The downdraft on the downshear side of the cloud was increased in intensity. These differences in the pressure field and draft structure remained very pronounced over 10 min following seeding. At that time, the tower which consisted mainly of ice crystals had a top about 3 km higher than in Experiment I. At one hour simulated time (18 min after seeding) the tower again was completely separated from the low levels and the intensity of the circulation had fallen back to the levels of Experiment I. Total precipitation was increased by almost 100% over Experiment I.

5. Conclusions

It should be noted that the results presented in this paper are of a preliminary nature and subject to revision after a more detailed analysis of the numerical experiments. At this stage, the main effect of seeding is found to be accelerated tower growth and an increase in precipitation, while the link to the subcloud layer remains unclear. The intensification of the downdrafts failed to initiate or sustain convection in this case study. The reasons for this are currently being reviewed and will be presented at the conference.

Acknowledgments

References

Clark, T., 1979: Numerical simulations with a three-dimensional cloud model: lateral boundary conditions experiments and multicellular severe storm simulations. J. Atmos. Sci., 36, 2191-2215.

Cotton, W.R., and G.J. Tripoli, 1978: Cumulus convection in shear flow - three-dimensional numerical experiments. J. Atmos. Sci., 35, 1503-1521.

_____, and _____, 1979: Implications of recent three-dimensional simulations of convective clouds to the dynamic seeding of clouds over Florida. Preprints, 7th Conference on Inadvertent and Planned Weather Modification, October 8-12, 1979, Banff, Alta., Canada.

Cunning, J.B., R.I. Sax, R.L. Holle, and H. Poor, 1979: Morphology of seeded clouds as determined from triple-Doppler radar - a case study, ibid.

Klemp, J.B., and R.B. Wilhelmson, 1978: The simulation of three-dimensional convective storm dynamics. J. Atmos. Sci., 35, 1070-1096.

Matsuno, T., 1966: Numerical integration of the primitive equations by a simulated backward difference method. J. Meteor. Soc. Japan, 44, 76-84.

Sax, R.I., D.M. Garvey, and F.P. Parungo, 1979: Characteristics of AgI pyrotechnic nucleant used in NOAA's Florida cumulus experiment. J. Appl. Meteor., 18, 195-202.

Simpson, J., 1980: Downdrafts as linkages in dynamic cumulus seeding effects, to be published in J. Appl. Meteor.

_____, R.H. Simpson, D.A. Andrews and M.A. Eaton, 1965: Experimental cumulus dynamics. Rev. Geophys., 3, 387-431.

_____, G.W. Brier, and R.H. Simpson, 1967: Storm fury cumulus seeding experiment 1965: Statistical analysis and main results. J. Atmos. Sci., 25, 508-521.

Stephens, M.A., 1979: A simple ice phase parameterization. M.S. Thesis, Colo. St. Univ., Fort Collins, Colo., 105pp.

Tripoli, G.J., and W.R. Cotton, 1980: A numerical investigation of several factors contributing to the observed variable intensity of deep convection over South Florida, under revision for J. Appl. Meteor.

APPENDIX 2

A Three-Dimensional Numerical Simulation and
Observational Analysis of an Intense, Quasi-
Steady Thunderstorm Over Mountainous Terrain

A THREE-DIMENSIONAL NUMERICAL SIMULATION AND
OBSERVATIONAL ANALYSIS OF AN INTENSE, QUASI-
STEADY THUNDERSTORM OVER MOUNTAINOUS TERRAIN

W.R. Cotton, G.J. Tripoli, K.R. Knupp

Department of Atmospheric Science
Colorado State University
Fort Collins, USA

1. Introduction

On 19 July, 1977, an intense, quasi-steady thunderstorm was observed by three Doppler radars, rawinsondes, and the NCAR Portable Automated Mesonet (PAM) over South Park, Colorado, during the Colorado State University 1977 South Park Area Cumulus Experiment (SPACE-77).

In this paper, we summarize the salient mesoscale features leading to the formation of the quasi-steady thunderstorm and the observed structure of the storm. The results of numerical experiments with the three-dimensional cloud model reported by Cotton and Tripoli (1978), Tripoli and Cotton (1980) and Cotton, et al. (1980) attempting to simulate the formation and structure of the observed storm are discussed.

2. Observations

2.1 Mesoscale environment and general echo characteristics

The 19 July regional synoptic environment was characterized by relatively weak-shear 5-10 m s^{-1} southerly flow at mid to high levels. Throughout the day, the NE transport of low-level moisture over Colorado resulted in early deep convection over NW Colorado and midafternoon deep convection over South Park. An analysis of the evolution of the 19 July South Park mesoscale features by George (1979) revealed a relatively complex, time-evolving pattern. During the initial stages, a north-south line of echoes was induced by a corresponding north-south line of low-level convergence, with 5-7 m s^{-1} westerly winds to the west, and 5-7 m s^{-1} easterly winds to the east. New convective cells 6-8 km in diameter typically formed periodically (10-20 min) on the line's southern (upshear) end and moved northward at 6-8 m s^{-1} through the line while slowly weakening.

The low-level flow and echo patterns at 1742 MDT (approximately 90 min after the line's formation) are portrayed in Fig. 1. At this time, airflow behind a southward-advancing meso-cold front was characterized by relatively strong northerly surface-winds (especially to the west of the line). The vertical structure of this post-frontal air mass exhibited significantly greater low-level shear of the horizontal wind ($\sim 10^{-2}$ s^{-1}) and relatively large low-level mixing ratios (~ 9g kg^{-1}). The total buoyancy of a parcel lifted from the surface was similar on each side of the front, although greater low-level negative buoyancy existed in

the cooler air. The post-frontal northerly flow remained over the western half of South Park for the ensuing 90 min. The increased low-level shear of the relatively shallow (≤ 1 km) airmass apparently altered subsequent storm structure and motion. One preexisting cell within the echo line's interior spawned a secondary cell which split and exhibited a diverging trajectory. Another storm, discussed in greater detail in the following section, rapidly intensified upon encountering the moist, northerly flow.

2.2 Observed characteristics of a quasi-steady storm (C11)

The most significant change in post-frontal storm behavior was the rapid intensification and organization of a relatively weak, multicellular cluster located on the southern end of the echo line. Prior to the arrival of the meso-cold front, this cell group exhibited a transient behavior in echo characteristics. Contrastingly, after the front's passage, the cell cluster rapidly intensified and consolidated within 30 min to become a heavy precipitating, quasi-steady storm which traveled $\sim40°$ to the left of the mean environmental cloud-level winds for the next 60 min.
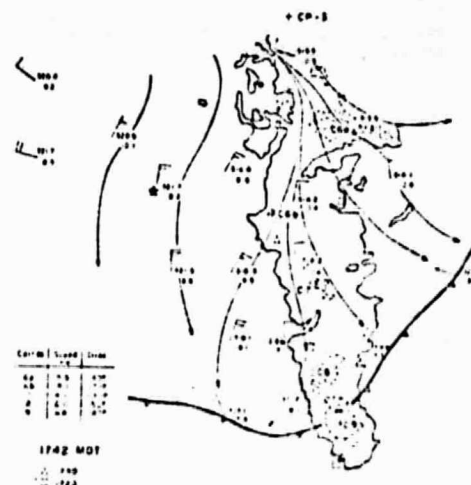

Fig. 1 Surface flow streamlines, mesonet parameters, and 1.5° CP-3 PPI echo contours (25 dBZ and 40 dBZ) at 1742 MDT. Trajectories of echo centroids are depicted. The 1710 vertical sounding location is denoted by star. (From George, 1979).

The salient features of the flow patterns within and adjacent to C11 during its steady period are portrayed in Fig. 2. Storm motion was directed towards the NW in response to continuous regeneration of precipitation within the propagating updraft U1, located above the gust front in the NW storm quadrant. The steadiness of storm circulation patterns is attributed to the constructive interaction of the NW-moving gust front with opposing low-level flow. The observed behavior is consistent with previous numerical experiments (eg., Klemp and Wilhelmson, 1978; Thorpe and Miller, 1978) which have elucidated the importance of wind shear profiles on storm motion and organization. Airflow at midlevels was characterized by accelerated flow around the updrafts and a weak flow wake region extending downstream. Anticyclonic vorticity peaking at midlevels (1.2×10^{-2} s^{-1}) was associated with updraft U1, while cyclonic vorticity was associated with flow around the updraft U2. Tilting of vortex tubes was a primary contributor to these patterns. High turbulence (Doppler radar inferred) was especially pronounced and persistent at midlevels along the southern and western storm quadrants. Estimated turbulent kinetic energy dissipation rates exceeded 0.4 m^2 s^{-3} within a highly sheared region separating an updraft and downdraft. Less intense turbulence was associated with midlevel relative storm inflow along the southern storm quadrant.

Doppler-derived draft patterns (Fig. 2) exhibited more complexity than corresponding reflectivity patterns. Updraft U1 had roots ahead of the gust front in the NW (downshear) and exhibited a reversal in tilt from lower to upper levels. Continuous northwestward propagation of U1 apparently governened storm movement. Analyzed maximum updraft speeds attained peak magnitudes of 20-30 m s^{-1} at upper midlevels (708 km AGL). A secondary, less intesnse and extensive updraft, with peak speeds of 10-20 m s^{-1}, was analyzed in the southern storm quadrant. Its forcing mechanism could not be resolved from the Doppler data or surface mesonet data. Diverging of low-level flow around the west side of the gust front and subsequent
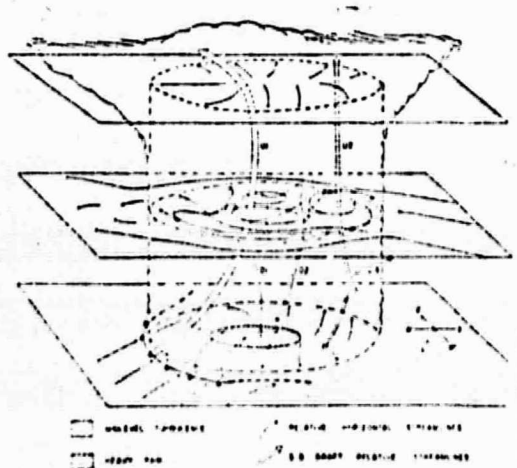
convergence along the southern flank, similar to what has been modeled by Tripoli and Cotton (1980) may have played a role. The analyzed downdraft circulations consisted of three cells or source regions which coalesced near the surface to produce a coherent cold air mass and associated gust front. Inferred downdraft initiating and maintenance mechanisms consisted of precipitation drag (D1) and evaporational cooling (D2 and D3). Flow around U2 was instrumental in producing downdraft D2.

One of the most striking characteristics of C11 was its copious production of precipitation. Of the 12 primary storm cells observed during a 4½-hour period within South Park, C11 contributed ~30% of the total precipitation. Such a large fraction was attributed to C11's quasi-steady organized circulation and relatively long lifetime. The peak measured rainfall rate (1855 MDT) was 190 mm hr^{-1}, corresponding to a maximum low-level reflectivity of less than 50 dBZ. Even higher rainfall rates may have existed after 1900 MDT since low-level reflectivity factors exhibited an increasing trend until 1937. Analysis of C11's radar echo characteristics revealed that areas of 40 dBZ and 45 dBZ echoes at 1 km AGL, as well as volumes enclosed by 40 dBZ and 45 dBZ echo surfaces attained maximum values at 1930. In contrast, updraft (and mass flux) magnitudes decreased slowly after attaining peak strength at 1900 MDT. Such a relationship implies that C11's precipitation efficiency increased with time.

Despite C11's dynamic vigor and organization, large hail was inferred absent because of the lack of significantly hign reflectivity (55 dBZ maximum). However, small hail and/or graupel may have reached the surface. The absence of large hail, together with the presence of high rainfall rates, implies that precipitation processes within C11 were extremely efficient. Analyzed airflow and reflectivity patterns suggest that such a high precipitation efficiency resulted from an organized recirculation of precipitation from the updraft at midlevels to that at low levels. Recirculating tranjectories were made possible by the large angle (~140°) between the midlevel and low-level wind vectors. Therefore, airflow and turbulent motions adjacent to the midlevel updraft would have transported precipitation from the updraft northward over the low-level inflow. The high precipitation efficiency also implies that the liquid water depletion concept advanced by Foote (1979) was occurring naturally with C11, where numerous particles reentered the downshear updraft (U1) in both liquid and solid form (this is substantiated by visual observations of a nebulous inflow sector). Thus, recirculation of precipitation elements explains (a) high rainfall rates, (b) lack of large hail, and (c) absence of a radar echo vault.

In summary, the change in low-level airflow affected storm-scale processes in two ways: (1) it altered storm dynamical processes by producing a quasi-steady updraft which governed storm movement; (2) the low to midlevel level directional wind shear promoted an organized recirculation of precipitation elements into the low-level updraft, thus modifying precipitation growth processes.

Fig. 2 Conceptual model of C11's flow patterns during its intense, organized storm stage.

3.0 Numerical Experiments

In order to gain a greater understanding of the dynamics responsible for the production and maintenance of C11, a three-dimensional numerical simulation of cumulus development in the observed 17 July, 1977 environment was performed. The improved CSU multidimensional cloud model summarized by Cotton et al. (1980) was used. This model utilizes an ice phase parameterization developed by Stephens (1979) in which mixing ratios of ice crystals and larger graupel particles are explicitly predicted.

Because the ultimate objective of this study is to use the model to gain further insight into the dynamical structure of C11, the basic state temperature, moisture and wind fields were specified initially from a late afternoon post-frontal sounding. A domain of 35 km square by 17 km high was selected with a uniform 750 m grid spacing. A convective circulation was initiated by the introduction of a low-level focused convergence field (see Tripoli and Cotton, 1980) producing a strong induced uplifting within an 8 km radius of the domain center. Surface moisture and potential temperatures were initially perturbed upward to the level of free convection in the region of maximum convergence so that downward acceleration produced by negative buoyancy would not destroy the perturbation before the cloud became self-sustaining. As a result, an intense cumulus circulation developed reaching 14.5 km MSL. The updraft, with a peak magnitude of 14 m s^{-1}, evolved from the initial upward motion and migrated to the southern quadrant of the storm. This migration can be explained by the findings of Tripoli and Cotton (1980; hereafter referred to as T-C), which showed that in the presence of strong initial low-level convergence, the perturbation updraft may become long-lived. Associated with vigorous well-rooted, initial disturbances was a surface pressure low. In some cases, T-C found that the pressure anomaly was intense enough to divert downdraft air beneath the updraft in a direction opposite to the downward transport of horizontal momentum. Thus the downdraft reinforced the initial updraft which in this case was located in the southern quadrant of the storm.

Because the updraft in C11 was, in fact, observed in the northern quadrant of the storm, it was decided to try a different approach to storm initialization. Storm C11 was observed to first develop in the prefrontal environment before taking on the characteristics of a steady state circulation subsequent to frontal passage. This earlier development took place along the southern flank of a convective line formed in conjunction with a preexisting mesoscale convergence zone. In addition, the low-level wind shear was opposite to that encountered later on. It was decided, therefore, to simulate convection first in the prefrontal environment and then artificially induce a frontal passage in the presence of mature convective cells.

To accomplish this, a new domain 45 km long in the north-south direction, 30 km wide in the east-west direction and 15 km high (18 km MSL) was used. A uniform grid spacing of 750 m

was again taken. Initially, a uniform surface mesoscale convergence of 0.27 x 10^{-3} s^{-1} (similar to observed) was imposed. A region of more vigorous vertical motion was imposed in the center of the southern 2/3 of the domain within a diameter of 8 km. The focusing function was slightly different than that of T-C in order to contain all compensating subsidence within a radius of 15 km, instead of over the entire domain. This was necessary because the perturbation is not centered in the domain. It was anticipated that with this initialization method, convection will develop in conjunction with the focusing, drift northward and develop new cells to the south as observed. The results show that indeed convection developed, drifted northward and some new convection was produced to the south. The initial forced cell reached 14.5 km MSL which can be compared to 15 km MSL observed in the prefrontal environment. Peak updrafts of 24 m s^{-1} were produced. No prefrontal estimates of vertical velocity were made from observations, however values of 25 m s^{-1} were observed in C11 after frontal passage. Precipitation of over 1.5 cm over a 3.5 km^2 area occurred primarily in the form of graupel. This is compared to observed values of 1.0 cm, although sampling stations may not have been located in the maximum zone. Fig. 3 shows the cloud water field at 2250 m above the ground level after 50 min simulation time. A loosely organized north-south pattern of convective cells can be seen.

Numerical experiments in progress at the time of this writing include an altered initialization algorithm designed to tighten up the
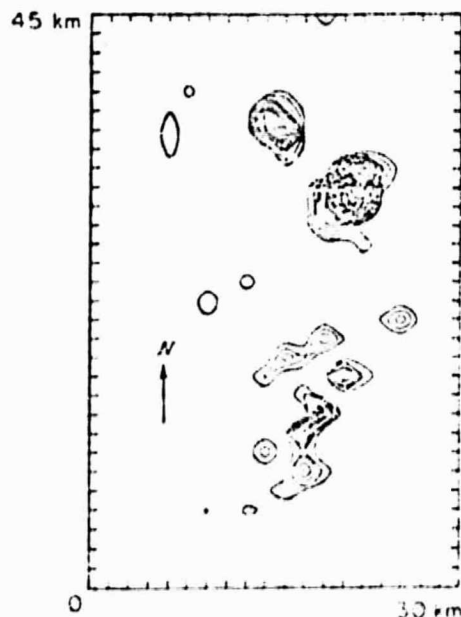

Fig. 3 Horizontal cross section at 2.25 km above ground with cloud water field contoured at intervals of .01 g cm^{-3}.

organization of the north-south line of cells. In addition, the passage of the ne..-cold front through the line of mature convective cells will be induced. The results of these numerical experiments will be described in the oral presentations.

4.0 Acknowledgments

5.0 References

Cotton, W.R., and G.J. Tripoli, 1978: Cumulus convection in shear flow - three-dimensional numerical experiments. J. Atmos. Sci., 35, 1503-1521.

Cotton, W.R., T. Nehrkorn, C.J. Tripoli and J.B. Cunning, 1980: A th e dimensional simulation of the dynamic response of a Florida cumulus to seed'.g. Preprints to the Third WMO Scientific Conference on Weather Modification.

Foote, G.B., 1979: Further aspects of the hail suppression problem. Preprint to Seventh Conference on Inadvertent and Planned Weather Modification, 180-181.

George, R.L., 1979: Evolution of mesoscale convective systems over mountainous terrain. M.S. Thesis, Colorado State University, Fort Collins, Colo., 160 pp.

Klemp, J.B., and R.B. Wilhelmson, 1978: The simulation of three-dimensional convective storm dynamics. J. Atmos. Sci., 35, 1070-1096.

Stephens, M.A., 1979: A simple ice phase parameterization. M.S. Thesis, Colorado State University, Fort Collins, Colo., 122 pp.

Thorpe, A.J., and M.J. Miller, 1978: Numerical simulations showing the role of the downdraft in cumulonimbus motion and splitting. Quart. J. Roy. Met. Soc., 104, 873-893.

Tripoli, G.J., and W.R. Cotton, 1980: A numerical investigation of several factors contributing to the observed variable intensity of deep convection over South Florida. Under revision for J. Appl. Meteor.